NPL
National Physical Laboratory

Report

NPL REPORT
DEPC MPR

Rheological characterisation Of filled materials: a review

M RIDES

NOT RESTRICTED

February 2005

dti
FUNDED BY THE DTI

National Physical Laboratory | Hampton Road | Teddington | Middlesex | United Kingdom | TW11 0LW
Switchboard 020 8977 3222 | **NPL Helpline** 020 8943 6880 | **Fax** 020 8943 6458 | **www.npl.co.uk**

Rheological characterisation of filled materials: a review

M Rides
Division of Engineering and Process Control

ABSTRACT

This report presents a review of measurement methods for the rheological, or flow, properties of filled materials focusing on polymeric materials and in particular on the measurement of slip flow that occurs in filled materials, predominantly through the development of a lubricating layer adjacent to the wall of the flow channel. It also describes models used for predicting the effect of filler on the viscosity of materials and presents the basis for unification of flow curves. The modelling and unification of flow curves can be used to facilitate the prediction and measurement of the rheological behaviour of materials.

ISSN 1744-0270

National Physical Laboratory
Hampton Road, Teddington, Middlesex, TW11 0LW

We gratefully acknowledge the financial support of the UK Department of Trade and Industry (National Measurement System Policy Unit)

Approved on behalf of the Managing Director, NPL,
by Dr M G Cain, Knowledge Leader, Process Materials Team
authorised by Director, Engineering and Process Control Division

CONTENTS

1 Introduction

This review primarily covers the measurement of the flow behaviour of multi-phase materials, but also covers aspects of materials modelling, specifically on constitutive equations for flow of filled materials. In particular the review focuses on the characterisation of slip flow of filled materials.

Reliable characterisation of the rheological behaviour of materials is important for many reasons, whether it is for developing new materials with specific flow properties, design of processes using rheological data for existing materials or for quality control of materials in production processes. The introduction of fillers can significantly affects the flow properties of the base material, with the effect becoming very significant at high filler levels. Fillers can be added to control flow behaviour (e.g. paints) and solid (or liquid) particles can be mixed as slurries (or emulsions) to improve handling and processing properties. Measurement and modelling can be complicated by the onset of phenomena not necessarily seen in the unfilled material, for example yield behaviour and slip flow. However, fillers can affect all aspects of the rheological behaviour of the material in a multitude of ways.

Filled materials cover a very broad range of materials from plastics to food, concrete to ceramic slurries, adhesives to liquid metals. Fillers may be added to reduce the cost of the material and/or to improve its performance either in processing or in service by changing its physical, mechanical (strength, toughness, hardness, impact resistance, dimensional stability), permeability, electrical, magnetic, chemical, thermal and rheological properties. Fillers, for the purposes of this report, refer to solid materials that are largely inert[1] but exclude particles having very large dimensions, e.g. continuous fibres. Furthermore, there is significant growth in interest in nano-fillers in polymers as evidence demonstrates that disproportionate benefits can be achieved by the addition of small quantities of filler. Obviously it is not possible to do justice in a single review of this nature to all filled materials. Therefore this report principally focuses on the measurement of highly filled plastics materials, although reference is made to other materials where this provides additional understanding to the measurement issues related to filled plastics.

2 Materials and flow phenomena

2.1 Introduction

This section briefly looks at the very broad range of materials that constitute filled materials, covering polymers, fillers and additives. It clearly demonstrates that with the large number of permutations of polymers, fillers and additives, filled polymers can be very complex materials. Mixing of filled materials can have an effect on the homogeneity of such materials and their properties: insufficient mixing may result in a lack of homogeneity, but a conflicting requirement will be to minimise the amount of mixing to, for example, minimise mechanical degradation. Furthermore, there is also a wide range of flow properties that can be measured in shear and in extension, including yield and slip flow behaviour, which can potentially be influenced by filler content. Thus, even restricting to filled polymeric materials it is clear that there are a significant number of permutations of factors affecting their rheological properties.

[1] Fillers may be considered inert on the bulk-scale but not necessarily on a surface-scale where interactions with coupling agents etc may occur.

Polymeric materials are very varied: they may be thermoplastic, thermosetting or elastomeric. Thermoplastics may be linear or branched, and amorphous, crystalline or semi-crystalline in nature, with significant variations in molecular weight even within a single type of polymer, e.g. polyethylene. Similarly, differences in thermosetting plastics and elastomers makes polymeric materials a broad and diverse range of materials with a similarly broad range of properties. Obviously, the rheological properties of the base polymer, e.g. its viscosity, will naturally affect the rheology of the mix.

2.2 Filler types

Many types of fillers are used in polymeric materials to modify physical mechanical properties, improve processing properties, improve durability, impart some functional behaviour (such as conductivity or magnetic properties) or to reduce cost. The types of fillers used depend on the property requirements and value of the material. Filler commonly added include toughening agents (e.g. rubber particles), inorganic minerals (e.g. calcium carbonate, talc, fly ash or gypsum), colouring pigments (including titanium dioxide, carbon black), magnetic agents (e.g. powdered ferromagnetic materials), conductive particles (e.g. powdered metals, silver particles), mechanical reinforcement (e.g. natural, glass or carbon fibres) or nano-fillers (e.g. clays or colloidal silica).

Fillers vary not only in type, but for any given type the filler may also vary in terms of its physical properties. Many fillers are natural in origin and consequently vary in properties. Properties that may affect how the filler contributes to the rheology of the mix include:

particle shape[2] (and distribution)
particle size (and distribution)
particle stiffness (e.g. rigid or flexible fibres)
surface topology and properties
surface chemical properties (surface treatment)
interfacial energy (wettability)
density (difference between matrix and filler – buoyancy effects)

and, not least, the amount of filler added, i.e. the volume fraction or concentration.

Obviously, the magnitude of the effect that some of these factors will have will depend on the properties of the base polymer.

2.3 Surface treatment and additives

In addition to the “solid” fillers, commercially available grades of filled polymeric materials also potentially contain numerous other additives. Even so-called unfilled polymers often have a number of additives that are used to control their thermal, rheological and mechanical properties. Additives in filled polymers, applied either to the filler or to the base polymer, include plasticizers (e.g. polyesters and phthalates), lubricants (e.g. silicone, stearates), stabilisers, filler surface modifiers (e.g. silanes, titanates, zirconates, zircoaluminates,

2 The filler particles shape may be predominantly 1 - dimensional, e.g. fibres or whiskers, 2 - dimensional, e.g. flakes or platelets, or 3 - dimensional, e.g. spherical or ellipsoidal

hydrophobic wetting agents), and pigmentation. All potentialy might have an effect on the flow properties of the material. Surface modifiers may be considered either as lubricants or, where they couple with both the filler and the matrix, as coupling agents. The complex package that often makes up the polymer must be taken into account in understanding its flow properties. An additional factor that might affect the behaviour of fillers and thus the materials they fill is the moisture content, which can vary depending on the conditions in which the materials are stored, handled and prepared. Examples of particularly water sensitive polymers are PBT, PET and PA.

2.4 Flow fields and flow phenomena

The effect of the filler on the flow will be different depending on whether the flow is steady, dynamic (oscillatory) or transient shear, or steady or transient extension, or some complex combination of these. Extensional flow itself can be broken down into further categories of uniaxial, planar, and equibiaxial. Furthermore, polymeric systems exhibit viscoelasticity and the effect of a filler on the viscous and elastic components of the dynamic viscosity will potentially differ.

In the flow of polymeric systems various phenomena may occur which will influence the rheological properties of the material, namely:

- particle interaction / particle motion (rotation)
- flocculation/de-flocculation/agglomeration
- mechanical degradation of filler
- particle depletion/migration e.g. away from the wall
- flow separation (e.g. squeezing out of continuous phase in contraction flows)
- electrostatic effects

Additional flow phenomena that occur in filled materials include:

- slip behaviour
- yield behaviour

The characterisation of the rheological behaviour of filled materials is further complicated by their potential time dependence. Being viscoelastic materials, the rheological properties of polymers can be time dependant and this is also the case with filled materials. The microstructure established in a filled material, e.g. agglomerations or flocs, may result in a time dependence of rheological properties due to the breakdown/formation of such structures during testing.

Furthermore, there is significant and clear evidence demonstrating that the surface finish and material composition of the die wall can have a significant affect on measured flow properties.

2.5 Mix quality

Consistent properties, whether they are rheological, mechanical or physical require that the mix is sufficiently homogeneous. However, like most processes, mixing is a compromise, in this case between maximising the performance of the material and minimising the costs. The performance of the material is often associated with the quality or homogeneity of the mix. The cost can be viewed in terms of the financial costs of production in terms of ingredients,

energy consumption, mixing time and production capacity, and also in terms of materials degradation, for example thermal degradation of the polymer or mechanical degradation of the filler. Mix quality will be affected by the physical, thermal and mechanical properties of the ingredients. For example, a higher viscosity polymer is more likely to break down particle agglomerations during mixing due to the higher stresses involved.

The reader is referred to Shenoy [1] for a detailed description of fillers and other additives used in polymers.

3 Definitions

The following definitions are based on the British Standard BS 5168 [2], Hadley et al [3] and Barnes et al [4]. For the original definitions and also further rheological definitions the reader is pointed to these references.

Filler
The discontinuous phase of a mixture.

Matrix
The continuous phase of the mixture.

Volume fraction (also known as phase volume) ϕ
The fractional volume of the filler to that of the mixture. It is expressed as a percentage of the total volume.

Note: It is important to express such a parameter describing the composition of the mixture on a volume rather than mass basis.

Maximum volume fraction ϕ_m
The maximum volume fraction that can achieve corresponding to the maximum packing density of the filler. It is expressed as a percentage of the total volume.

Relative viscosity (also known as viscosity ratio) η_r
The ratio of the viscosity of the mixture (suspension) to that of the continuous phase.

Shear thinning
A reduction in viscosity with increasing rate of shear in steady flow (the opposite of shear thickening) BS 5168 [2].

Shear thinning is also known as pseudoplasticity, but this term is deprecated. BS 5168 [2] refers to pseudoplasticity as time dependant shear thinning with no yield stress, whereas Hackley [5] describes it as an alternative word for shear thinning. However, Hadley et al [3] suggest that the use this term for shear thinning should not be encouraged.

Yield stress σ_y
The stress corresponding to the transition from elastic deformation (below the yield stress) to plastic deformation (above the yield stress). It is expressed in Pascals (Pa).

Thixotropy
A reversible time-dependent decrease in viscosity at a particular shear rate or shear stress **(**the opposite of negative- or anti-thixotropy).

Recovery is unlikely to be instantaneous on removal of the stress since inter-particle networks will take time to reform.

Additional terms are used in the literature to describe rheological behaviour, but comparison of documents indicates variation in their definitions. The following are presented here:

Rheopexy
The solidification of a thixotropic material by gentle and regular motion (BS 5168 [2] and Hackley [5]). However, BS 5168 [2] and Barnes et al [4] indicate it is used as a term equivalent to negative or anti-thixotropy.

Rheomalaxis
An irreversible decrease of viscosity during shearing, attributed to permanent changes in the material structure (Hackley [5]). BS 5168 [2] refers to rheolmalaxis as the loss of consistency – i.e. ability to resist permanent deformation.

4 Measurement techniques

4.1 Introduction

As can be seen from the above sections the permutations in the manufacture of filled materials are many, and many of the parameters, e.g. filler size distribution, affect the rheological behaviour of the materials. This review focuses on the issues of measuring the flow behaviour of filled materials, in particular their slip flow behaviour.

The rheological behaviour of filled materials has been investigated using a range of techniques: capillary die and slit die extrusion rheometry, melt flow rate testing, rotational rheometry using a wide range of geometries, oscillatory rheometry, extensional rheometry, torque rheometry, squeeze flow techniques, oscillating probes, and alternative techniques not always associated with rheological characterisation, for example ultrasonic or acoustic transmission.

To obtain higher shear rates in-line extrusion rheometers can potentially been used, for example Coates et al [9]. Similarly, screw extruders and instrumented mixers (torque rheometers) can be used to measure rheological behaviour [10]. Squeeze flow techniques, mimicking the compression moulding process, have been used to characterise highly filled thermosetting materials, e.g. glass-fibre and particulate filled unsaturated polyester dough moulding compounds. Silva-Nieto [11], using the squeeze flow technique, determined the flow behaviour parameters, including yield stress values, by least squares fitting of the experimental raw data. A difficulty with ultrasonic and acoustic techniques is in relating the properties measured at very high frequencies and low strains to the performance of the material in the process, equivalent to significantly lower frequencies and higher strains.

Textured surfaces for plates in rotational/oscillatory rheometry and for extrusion dies in capillary and slit rheometer have been used to disturb the development of a slip layer, which affects the measured properties. These techniques are discussed in Section 5.5 on slip.

4.2 Particle size issues

With the established rheological techniques (extrusion and rotational/oscillatory rheometry) a particular issue that needs to be addressed when measuring filled materials, but is not always done so, concerns the filler particle size. A major issue in carrying out valid rheological measurements of filled materials is the identification of the necessary gap size to use to ensure that particle size, or in the case of agglomerates the agglomeration size, does not affect the measurements, i.e. that the results are not test geometry dependent. However, this requirement conflicts with other potential requirements, e.g. the need for data at appropriate shear rates. Polymer processing tends to be a high shear rate process and to avoid extrapolation of low rate data it is necessary to obtain data at such high rates. In capillary extrusion rheometry, controlling the diameter of the extrusion die is the main control the operator has over the shear rate range obtained. In capillary rheometry the shear rate is inversely proportional to the third power of the die radius. In comparison, the shear rate is only linearly proportional to the piston speed. Thus to obtain data at high shear rates small die diameters need to be used. A further consideration is that plastics are often processed through small (thin) channels, for example in injection moulding, in which size effects (e.g. wall slip) may be significant. It may then be more appropriate, if slip is not modelled, to use dies in capillary rheometry testing of similar size to the channels for which modelling is required. This will avoid the need to extrapolate the flow behaviour of the material determined using large-sized dies to that in small-sized mould channels.

Hackley [5] commented that for testing coarse-grained materials in extrusion-based devices the orifice (die) diameter must be 3 to 5 times larger than the maximum particle size. This was supported by Atanasio et al [12] who claimed that provided the width of the flow field is more than 3 times the length of elongated particles then agreement between capillary and Couette rheometer measurements were obtained. Similarly, Collyer [13] concluded that if the ratio of the largest dimension to the edge gap in rotational rheometry is not more than 1/3 then the effect on measurements will be small, though he later commented that to obtain greater accuracy larger ratios may be required. Lauger et al [14] commented that gap sizes should be of the order of 10 times the largest particle size. Similarly, Barnes [15] identified the following criteria for suitable gap sizes for testing of filled materials, but for highly filled materials he suggested that ratio of particle size to gap size should be smaller.

Filler content (% volume)	**Particle to gap ratio**
25%	Filler particle size < 0.1 gap size
50%	Filler particle size < 0.01 gap size

However, there are instances where rheometry measurements can be carried out with critical gap size less than particular particle dimensions, for example in the case of extrusion testing of fibre filled materials where the fibres have a length several times that of the capillary die diameter [16]. Such materials can be tested due to the alignment of fibres in the flow direction and also due to the flexibility of the fibres. However, rheological testing of, for example, glass-fibre filled materials can result in degradation of the fibre length and this itself changes the rheological properties of the material being characterised [16]. Such mechanical

degradation of the filler further complicates the characterisation as it can have a similar affect to that of orientation induced by flow.

4.3 Issues specific to rotational and oscillatory flow rheometry

In steady shear (continuous rotation) or dynamic (oscillatory) testing issues related to the particle (or agglomeration/floc) size relative to the gap size must be considered, as discussed above. Furthermore, to obtain reliable dynamic measurements of the elastic (*G'*) and viscous (*G"*) components of modulus in order to compare materials it is important to test in the linear elastic region of the material. For filled materials it can be difficult, if not impossible, given the operating limits of the instrument, to accurately determine the strain limit of the linear viscoelastic region within which reliable, comparable linear viscoelastic *G'* and *G''* data should be determined. Thus, unless it is clearly demonstrated that data have been obtained in the linear viscoelastic region, through the execution of strain sweeps, comparison of the behaviour of different materials with, for example, different volume fractions of filler can be problematic.

For steady shear testing using a rotational rheometer the normal approach is to use a truncated cone and plate geometry in which the virtual peak of the cone (virtual because of its truncation) contacts the surface of the flat plate. This ensures that the shear rates are uniform throughout the test region, and thus the assumptions made in the method of analysis are valid. However, the use of a small truncation may cause problems as the truncation is normally small, typically of the order of 0.05 mm to 0.2 mm due to the need to keep the cone angle small. Cross et al [17] have addressed this issue by using a displaced cone method and also a recessed (annular) cone and plate geometry. In the first instance the cone geometry is held at a greater distance from the flat plate, and in the second the central apex region of the cone is recessed and therefore has little effect on the measurement. Cross et al [17, 18] have also extended the displaced steady shear cone analysis to the parallel plate geometry by assuming a zero cone angle. Although they indicate that the method is suited for testing suspensions they validated it using a polyisobutylene - decalin solution, although later reference was made to successful measurements on glass-fibre in polyol slurries for which the use of conventional geometries had proved unsuccessful.

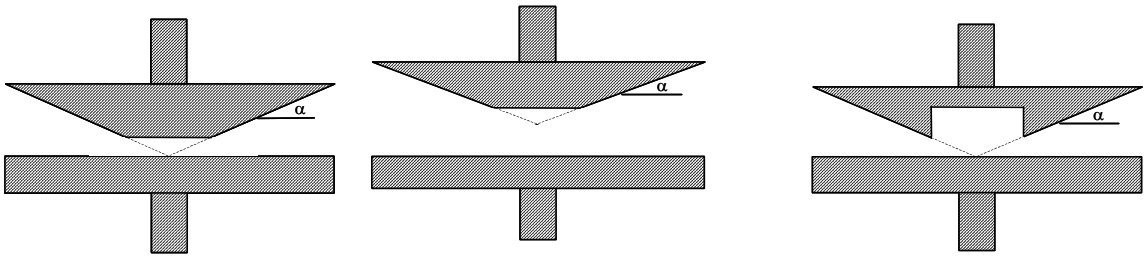

Figure 1: Normal truncated, displaced truncated and recessed (annular) cone and plate geometries

Couette geometries (concentric cylinders/cup and bob in rotation) are not typically used for polymer melts. However, Macosko [19] commented that for concentrated suspensions slip may occur at the walls of the concentric cylinders. One method to overcome this is to use a rectangular-vaned bob in a large reservoir so that there is no wall against which the fluid slips. Such vanes and also other vane geometries, e.g. H-shaped rotated about the central vertical

axis, are used, for example, in concrete testing [5, 20]. For heavily filled materials with strong shear thinning ($n < 0.5$) the fluid between the vanes effectively rotates as a solid cylinder, and there are no complicating issues with a small gap to consider. However, for heavily filled materials one must still consider whether a slip plane within the fluid is set up in the rotating system at a radius equal to the tip of the vanes due to particle migration. Such a layer could be assessed through study of the transient behaviour of the materials from start up of the test.

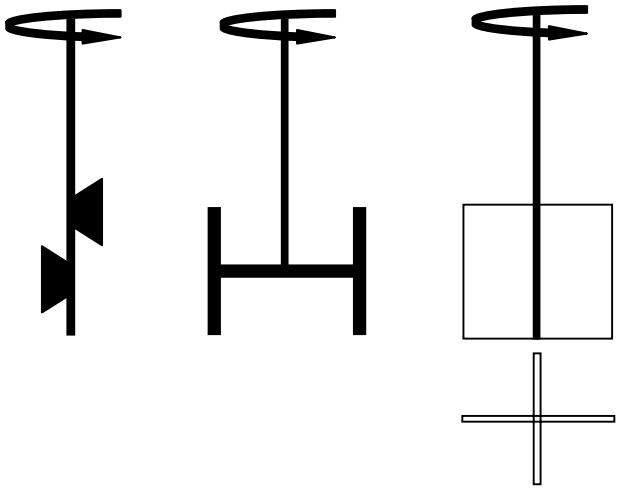

Figure 2: Various vane geometries used in rotational testing (Tattersal, H and double vaned)

Falling ball techniques [21] have also been used to measure the rheological behaviour of suspensions. However, due to the potential opacity and high viscosity of filled systems and the technique providing only very limited information on flow behaviour, the value of the method is limited. A similar approach is presented in [14] in which the ball, immersed in the fluid, is attached off-centre to a rotational rheometer drive. The ball is moved in a horizontal circle using the rheometer to measure both torque and speed. However, as with all invasive measurements of heavily filled materials, the shear history of the material can significantly affect the measured behaviour. In such techniques, and the various vaned geometries described above which in essence are the same technique with a different geometry, the measurement of unsheared material is limited to at most a single revolution or in the case of a double-vaned geometry a half revolution. Continuing the rotation will result in previously-sheared material once again being tested. The use of two vanes is preferable as it cancels out any bending moments on the rotor spindle that can affect its performance and calibration and increases the torque, but reduces the angle of rotation permitted before testing in pre-tested material.

4.4 Measurement issues with high aspect ratio fillers

The measurement of fibre-filled materials can be particularly difficult as the fibres are oriented by the flow field, e.g. in the entrance region of capillary rheometers where the orientation is due to the strong extensional flow field, or potentially in loading/compressing the sample in a rotational rheometer [22]. On the other hand the shearing flow in the die tends to randomise the orientation as the fibres tumble. Ausias et al [23] reported that orientation induced by pre-shearing short glass-fibre filled PP samples using a rotational rheometer affected their subsequently measured dynamic viscosities. However, they commented that the

shear flow occurring during oscillatory rheometry was itself not sufficient to cause orientation.

Electrical or magnetic fields can cause alignment of mobile particles in suspensions. Electrical fields orientate polarisable particles suspended in non-polar matrices in the direction of the applied field. Varying the electric field will alter the viscosity of these electro-rheological fluids. Magneto-rheological systems respond to magnetic fields. Potente [24] reported that orientation of fillers during flow, induced by the application of a magnetic field to flowing PA-6 polymer containing a magnetic filler (Strontium ferrite in the form of hexagonal platelets, 1-2 μm average size), significantly affected the measured viscosity. The application of the magnetic field perpendicular to the flow direction (presumably causing orientation in that direction) resulted in a reduction in shear viscosity by up to 50%. Potente [24] also reported that the shear viscosity data presented indicated that the material became more temperature dependant with increasing filler content.

Separation of the filler phase from the matrix can occur in rheological testing, not just in the context of particle migration from high shear rate regions in the proximity of a wall as discussed in the section on slip, but also in the context of separation in flow through an orifice as occurs in extrusion rheometry. This effect has been observed in testing of fibre-filled materials, for example by Rides [6], Murty et al [7] and Maschmeyer and Hill [8], and is more predominant at lower flow rates for a given geometry. Murty et al [7] report that to avoid jamming of fibres in the entry region in extrusion rheometry the viscosity of the carrier matrix must be greater than a critical value which is a function of the fibre size and volume fraction and also decreases with increasing gap width. Rides [16] has observed that the log-jamming effect, and also the noise in the extrusion pressure trace, can be reduced by the use of conical entry geometries which “smooth” the flow into the die.

5 Rheological behaviour

5.1 Introduction

Not surprisingly there is a significant quantity of work reported in the literature on the rheological characterisation of filled materials. This review does not attempt to cover them in detail by reporting on the behaviour of individual filled materials but to draw out the main measurement issues. Shenoy [1] and Barnes [15] presented comprehensive reviews of the rheological behaviour of a wide range of filled polymers.

In summary, the following broad generalisations of the effects of fillers on the rheological properties of polymers are made.

5.2 Shear viscosity

Factors that affect the shear viscosity of filled systems are numerous. Barnes [15] concluded that low concentrations of fillers increase the shear viscosity of polymers, and that long fibres result in greater shear thinning behaviour. High concentrations of filler resulting in interactions can result in an apparent yield behaviour. Barnes et al [4] commented that one effect of increasing filler content on shear viscosity is to increase the viscosity value at which the Newtonian plateau occurs. This can result in a Newtonian plateau for filled materials that

is very high and occurs at very low rates only and can thus be difficult to determine by measurement. This can be misinterpreted as an apparent yield phenomena (see Section 5.6 on yield).

Shenoy [1] concluded that shear and extensional viscosity exhibit similar trends with filler content. He commented that the addition of fillers increases the viscosity, the effect being greatest for 1-D fillers, then 2-D and least for 3-D fillers, and that rigid fillers have a greater effect than flexible fillers.

The filler size distribution effects viscosity: a disperse distribution having a lower viscosity than a less disperse distribution of equivalent volume fraction. This can be accounted for by consideration of the maximum packing volume for each of the filler types, which will be greater in the case of that with a more disperse distribution, and, for example, the MPK model (Section 6.1) which gives viscosity as a function of both the volume fraction and maximum volume fraction. Agglomerations, by capturing fluid and increasing the effective volume fraction, can result in an increase in viscosity by similar argument. Agglomerations can be induced or destroyed by flow. Particle interactions can depend on particle shape and effects of particle interactions can be more significant with high aspect ratio fillers than with near spherical fillers. Dealy [22] commented that particles greater than 10 microns have little tendency to aggregate and their effect on flow is purely hydrodynamic, whereas particles of sub micron size are affected strongly by attractive forces. Degradation of fibres due to testing and its effect in reducing the shear viscosity was clearly observed by Tsao et al [25].

Wang et al [22] commented that the effect of filler on shear viscosity was most significant at low rates, with the effect being negligible at high rates. Examination of their results indicated that the effect of filler loading was almost two decades at 10^{-3} s^{-1} but at 1 s^{-1} was still of the order of a factor of three for volume fraction loadings from 0% to 30%. The effect of volume fraction on shear viscosity decreased as shear rate decreased: the effect was most significant in the Newtonian plateau region. Once in the shear thinning region there was a tendency for the difference in shear viscosity of materials of different volume fraction loadings to decrease but that rate of decrease was small [26, 27]. In modelling the rheological behaviour of such materials, constitutive models that yield a shear rate dependence of the effect of filler on viscosity are obviously required for accurate description of the materials. However, this is not usually the case - the effect of filler on viscosity is normally taken to be independent of shear rate.

Wang [28] reported that for calcium carbonate filled PP, thixotropic behaviour was observed in testing materials with a volume fraction in excess of approximately 20%, commenting that the thixotropic effect increased in magnitude with increasing volume fraction.

5.3 Extensional viscosity and entrance pressure drop

The majority of results presented in the literature are on shear flow characterisation of materials, whether by extrusion or rotation rheometry. However, entrance pressure drop values determined from capillary rheometry measurements can be used as an indicator of extensional viscosity [6, 29-33]. Entrance pressure drop values are increased by the addition of filler, with very significant increases when those fillers are long fibres [6]. The effect of fibrous fillers is significantly greater on the entrance pressure drop in capillary rheometry than on shear viscosity [6]. Maschmeyer et al [8] emphasised the significant effect that fibre length has on rheological properties. This is reflected in the theories of Batchelor [34] and Goddard

[35] in which the addition of fibres significantly increases the extensional viscosity of the base polymer, and this is anticipated to be the case for all fillers of high aspect ratio. However, Dealy [22] has commented that fibres have been shown to both increase and decrease entrance pressure drop. Degradation of glass-fibres due to mixing has been shown to affect entrance pressures much more significantly than shear viscosity [6]. Rides [16] observed that additional mixing actually increased entrance pressure drop values due to breakage of glass-fibre bundles: this effect being greater that the opposing effect due to a reduction in fibre length. Barnes [15] commented that the addition of fibres results in a significant increase in the value of extensional viscosity, reflecting the effect on entrance pressure drop values.

5.4 Viscoelasticity

In summarising the effect of fillers on viscoelasticity, as characterised by the shear storage and loss moduli (*G'* and *G'')* for linear viscoelasticity and the first and second normal stress differences (N_1 and N_2) for non-linear viscoelasticity, Barnes [15] commented the viscoelasticity increases for low concentrations (non-interacting) of spherical particles. The increase in *G'* may not be a large as that in *G''* therefore resulting in a relative decrease in the ratio of elastic to viscous behaviour, i.e. the material becomes relatively less elastic. Similarly, the non-linear viscoelasticity of the material, as given by N_1/σ, may decrease slightly. However, Dealy [22] commented that rigid particle fillers can decrease N_1 values. Shenoy [1] commented that White at al [36] showed that fibres generally increased N_1 and non-fibrous particles decreased N_1 for filled PS, based on rotational rheometry measurements. Walberer et al [37] concluded that the effect of filler on *G'* and *G''* depended on the molecular weight of the PDMS polymer and the test frequency: increasing *G'* and *G''* values with frequency for low molecular weight but not high molecular weight materials. Walberer et al [37] interestingly also used an oscillatory compression technique and obtained good agreement with oscillatory rotation results. The addition of long fibres resulted in significant increases in all parameters [15, 22]. Dealy [22] commented that N_1 is related to the stiffness and length of the filler fibres. Shenoy [1] commented that the effect on linear viscoelastic behaviour is the same as that for shear viscosity. However, and as mentioned elsewhere (Section 6.4), it was observed that the Cox-Merz rule typically does not hold for filled systems [38].

The relative decrease in elasticity as described above was mirrored by the predominant effect of fillers to reduce extrudate swell and reduce recoverable shear strain [15, 22]. Delay [22] commented that the effect was the same for fibre as well as non-fibre fillers, although for long fibres and short dies very high extrudate swells can be observed but are considered to be due to the elastic deformation of the fibres in the die entry region.

An intercomparison of oscillatory rheometry measurements [39] of a talc-filled polypropylene-based copolymer clearly demonstrated the high scatter in results for the shear storage and loss modulus (G' and G'') values that can be obtained. The results indicated a 10% standard deviation for the unfilled material and values ranging from 15% to 60% for the filled material (although not stated the filler volume fraction is thought to have been 30%).

5.5 Slip flow

5.5.1 Slip flow mechanisms

There are two likely mechanisms for slip in polymer flow. In filled materials the development of a resin-rich layer adjacent to the wall due to particle depletion acts as a lubricating layer

with the resultant apparent "slip" behaviour. Alternatively, the polymer looses adhesion with the wall and slip occurs. Wall surface texture is known to influence slip behaviour [68-74].

Tuinier at al [40] modelled the effect of depletion of polymer in a solution near a wall on slip flow behaviour. They commented that slip effects were expected to increase with increasing polymer concentration beyond the semi-dilute regime. Modigell et al [41] showed, using NMR imaging of suspensions of PMMA spheres in a density-matched sugar solution, that the spheres migrated from regions of high shear rate to regions of low shear rate. Macosko [19] commented that the migration is greater for higher shear rates. Yilmazer et al [42] reported that migration of filler away from the wall in capillary flow increased with increasing shear stress resulting at high flow rates with 'effective viscosities' of filled materials approaching those of the unfilled materials. Kalyon [43] commented that slip of 63% filled fluids was due to the formation of a fluid-rich lubricating layer at the wall. As a consequence of such particle migration, the velocity profile is significantly affected: the migration results in a steep velocity gradient near the wall with the majority of the material flowing as a plug, which can be interpreted as slip. Cohen et al [44] analysed such behaviour using thermodynamic diffusion modelling and obtained reasonable agreement with experimental data.

The surface finish of rheometer plates or dies has been observed to affect slip behaviour, as discussed in more detail later (5.5.3). Aubry et al [45], using steady shear rotational rheometry with smooth and textured plates, concluded that slip in polymer solutions is due to destruction of network structures in the region near the wall. However, the apparent slip was not seen when using textured plates. Chen et al [46] reported that slip behaviour of low density polyethylene was influenced by both the material of construction and by surface roughness. No-slip was observed for aluminium whereas slip was observed for glass, copper and stainless steel, and slip decreased as roughness increased. Piau et al [47], using steel and PTFE-coated dies for extruding polybutadiene, observed significant differences in the apparent slip behaviour between the dies, with significant slip and improved extrudate surface finish in the case of the PTFE coated die. Piau et al [47] commented that the slip behaviour of polymers is related to the surface energy of the die wall: PTFE has a low surface energy compared with steel and slip is enhanced by it.

5.5.2 Mooney method for characterising slip flow

The onset of slip during a rheometry test should be apparent from a discontinuity in the shear stress – shear rate curve. However, if slip occurs at all the shear stress values obtained during the test then slip will not necessarily be apparent from a single die test. A second test using a different die diameter will lead to an apparent dependence of shear viscosity on the die diameter from which slip can be inferred. In the presence of slip, use of a smaller die will produce lower apparent viscosities at equivalent apparent wall shear rates. This approach of using capillary dies of different diameter to determine the slip velocity was first developed by Mooney [48]: the analysis for capillary extrusion rheometry data is presented in Appendix A. Mooney [48] also presented the analysis for testing using the Couette geometry in rotation following the same principles. Taking a different perspective, Macosko [19] commented that by extrapolating the viscosity as a function of die diameter to infinite diameter the "true" shear viscosity of the fluid can be determined.

Yoshimura et al [49] presented an improved method for Couette geometries utilising only two measurements, and the analysis for parallel plate geometries, as well as the analysis for the Mooney method for capillary geometries. The precision of the method has not been

demonstrated and under certain circumstances negative slip velocity values have been obtained which are obviously nonsensical [16]. These negative slip values could be attributed to the flow being more parabolic at higher flow rates (stresses) than at lower flow rates. At the low flow rates the stresses are insufficient to cause significant disentanglement of the fibres/filler resulting in plug-like flow behaviour. At higher flow rates, disentanglement occurs resulting in a more parabolic flow. Alternatively, at lower rates greater separation of the resin from the material occurs, as has been observed in the entry region of capillary rheometers, resulting in more efficient lubrication of the flow. The consequence of this is that the flow appears more like "slip flow" at lower rates than at higher rates. When interpreted using the Mooney analysis negative slip velocities were obtained [16]. Negative slip velocities have also been identified using capillary rheometry and the Mooney approach by Mendez-Sanchez et al [50] who suggested that it might be the result of flow-induced phase orientation effects. Similarly, Leblanc et al [51] obtained negative slip values for filled rubber compounds but associated it with the compressibility of the material. They commented that rubbers are more pressure sensitive than unfilled polymers and that compressibility has the opposite effect on the measurement of viscosity to that of slip. Thus the apparent negative slip was potentially due to the material's compressibility. Hagstrőm [52] identified that the Mooney method failed for extrusion rheometry testing of PVC using a slit die and an oscillatory rheometer, as slip velocities greater than the average flow velocity were obtained. Fleming [53] commented that difficulties may be experienced using the Mooney approach for materials that degrade rapidly due to different residence times in the barrel, and reported that several workers have developed refinements to the Mooney approach to address the issues of too high a slip flow or negative slip flow [54-59].

Hagstrőm [52] presented the analysis for the use of slit dies for determining slip velocity. It follows the same approach as Mooney [48] for capillary dies except that the apparent shear rate $\dot{\gamma}_{ap}$ is plotted as a function of the reciprocal of the slit thickness ($1/H$) for constant shear stress values. The gradient of the plot is expected to be linear with a value equal to six times the slip velocity u_s.

$$6u_s = gradient\ [\ \dot{\gamma}_{ap}\ versus\ 1/H, for\ constant\ shear\ stress] \qquad (1)$$

Kalyon et al [60] developed a variable gap in-line rheometer mounted on a screw extruder in which the gap could be adjusted using stepper motors. This provides a convenient facility for studying slip flow following the Mooney approach.

Aubry et al [45] and also Yoshimura [49] reported the method for rotational rheometry using parallel plates, plotting the apparent shear rate at the plate rim ($\dot{\gamma}_{ap}$) as a function of the reciprocal of the gap ($1/h$) for constant shear stress. The resultant plot is expected to be a straight line with a gradient equal to twice the slip velocity.

$$2u_s = gradient\ [\ \dot{\gamma}_{ap}\ versus\ 1/h, for\ constant\ shear\ stress] \qquad (2)$$

A benefit in using rotational rheometry is that controlled stress instruments are widely available and thus there is no need to interpolate data to obtain data at constant shear stress. Collyer et al [13] commented, however, that slip in parallel plate rheometry is mathematically equivalent to setting a gap height that is too high and reported that in work by Henson et al [61] using parallel plate rheometry, the measured slip was equivalent to a 10 μm error in gap

setting. Therefore, accurate gap height setting is critical for the determination of slip effects in rotational rheometry.

Park et al [62] used the Mooney approach for determining slip using a rotational rheometer but added that for a system in which there is a thin lubricating layer the thickness δ of that layer can be estimated by the expression:

$$\delta = \frac{u_S \eta_S}{\tau} \tag{3}$$

where u_s is the slip velocity, η_s is the viscosity of the lubricating layer and τ is the shear stress. The viscosity of the lubricating layer is unknown but can be assumed to be equal to the viscosity of the matrix (fluid).

Yeow et al [63] presented an inverse solution to the determination of shear viscosity and slip velocity from capillary rheometry data without assuming a constitutive form between relating slip velocity and shear stress to shear rate. Good agreement of derived values was obtained using data presented in the literature, but it highlighted difficulties in the determination of the critical shear stress above which slip occurred. This was reported as being an issue both for the inverse approach used and also for the Mooney approach. The approach could also be used to determine the yield stress, given appropriate data [63]. Such an approach may prove valuable in addressing the issues identified above of negative slip velocities or excessively high slip velocities due to the limitations of the Mooney approach.

Graczyk et al [71] used capillary rheometry with rough dies, flow visualisation and a twin capillary method introduced by Gleissle et al [72] to study slip of aluminium oxide-silicone oil pastes. The twin capillary method is basically the same as the standard Mooney capillary die method. However, it uses two dies of different diameter but the same *L/D* ratio and the extrusion pressure is controlled to obtain constant and equal stress conditions in each die. The flow rates in each die are measured. It thus avoids the need to interpolate to obtain shear rates as specified shear stress values. However, the entrance pressure losses should be negligible otherwise a Bagley correction [73, 74] for entrance effects is required. They concluded that the Mooney and twin capillary (constant pressure) method gave unrealistically high values. They suggest that the measurements are influenced by the entry region to the dies resulting in fully developed flow being established some distance from the die entrance and that the size of the effects differs for the different diameter dies used.

Yilmazer et al [64], in testing a 60% by volume filled suspension, identified that at high flow rates the flow was dominated by slip rather than shearing flow. Similar observations were made by Jiang et al [65] for hydroxypropyl guar (HPG) gels. However, slip velocities in excess of the average velocity for the flow were calculated indicating failure of the Mooney analysis. Both reported that the slip velocity data fitted the power-law expression reasonably well over a limited range of shear stresses:

$$u_s = a\ \tau_w^{\ b} \tag{4}$$

where *a* and *b* are constants and τ_w is the wall shear stress. This expression has also been used by Yilmazer [42] and gave a good fit to data. Both parallel plate and capillary methods were used to determine the slip velocity following the Mooney approach [48]. Although there was

no overlap in shear stress of data from the two methods the shear stress at the upper end of the rotational testing was similar to that at the low end of the capillary rheometry testing. Values for the slip velocity in this region were similar, although the gradients of slip velocity versus shear stress were possibly different for each of the test methods. The scatter in slip velocities was greater for those obtained by the parallel plate rotation method. Yilmazer [42] presented a further modification to the above equation of the form:

$$u_s = a\ (\tau_w - \tau_s)^b \tag{5}$$

where τ_s is the critical shear stress below which no slip occurred. However, examination of the data for a 60% filled suspension did not suggest that this latter equation gave a significantly improved fit to data than the former. The slightly improved fit, due to the change in gradient mentioned above coinciding with the change to the other technique, may possibly be due to reasons associated with the use of different techniques rather the second equation being a more realistic model.

Howarth et al [66] showed that for $Mg(OH)_2$ and talc filled PP and PE, using capillary rheometry and the Mooney approach, the slip behaviour is affected by the filler level. They proposed a model for the slip velocity of the form:

$$u_s = \left[\frac{\tau - \tau_c}{k(\phi)} \right] \tag{6}$$

where k is a slip coefficient that is dependant on the filler level ϕ and τ_c is a critical stress above which slip occurs. Values for τ_c typically ranged from 120 kPa to 220 kPa and the slip coefficient from 0 to 3.8.

Ahn and White [67], using the Mooney approach of different die diameters for capillary rheometry, showed that small quantities of an additive (e.g. 1% of octadecanoic acid and zinc stearate) can lead to slippage in flow of polyethylene (PE) and polypropylene (PP) originating from loss of adhesion to the die wall, but that such effects were minimal with polystyrene (PS), poly methyl methacrylate (PMMA) or polyamide-12 (PA-12). It was suggested that this is due to the lower polarity of the PE and PP compared with the PS, PMMA and PA-12 and that, due to their lower polarity, the PE and PP is preferentially replaced at the wall by the lower molecular weight additives thereby creating a slip layer. Macosko [19], in summarising, commented that slip in polymer melts occurs at a wall shear stress of approximately 10^5 Pa.

5.5.3 Surface Texture

The effect of texture of the wall on slip flow behaviour has been investigated by several workers, some of which is reported earlier. Knappe et al [68] reported that slip of unplasticised PVC, measured using slit dies of different thicknesses, was observed for smooth dies but was disrupted for textured dies. They suggested that this behaviour was due to the presence of a thin lubricating layer caused by flow-induced diffusion. Malvern Instruments Application note [69] described steady shear rotational rheometry testing on low viscosity suspensions and concluded that the use of roughened (serrated) geometries appears necessary to overcome slip effects. Wear of the die surfaces in uPVC extrusion, thought to be due to the titanium dioxide filler, resulted in observed reductions in the required extrusion pressure [70].

5.5.4 Flow Visualisation

Flow visualisation techniques using tracers, e.g. pigment, have been used to study the flow of opaque systems, as optical techniques suitable for transparent materials are unsuitable for heavily filled materials, e.g. [16, 71]. Atwood et al [75] used hot-wire anemometry to determine slip phenomena in HDPE claiming it can sense the transitions from slip to no-slip conditions. The method has advantage in that it can be used for opaque materials though it suffers from the fragility of the probes, viscous heating and flow field disturbance effects and from the need to calibrate to correlate temperature response of the hot-wire with melt velocity.

5.5.5 Slip and product quality

The role of slip or stick-slip in melt instabilities characterised by sharkskin or melt-fracture has been investigated by various workers over the last few decades. Slip appears to significantly modify the extrudate sharkskin and fracture behaviour, for example Piau at al [47] suggested that improved performance of extrusion processes could be achieved through modification of the die finish. However, the origins of such instabilities are still debated.

.

5.6 Yield behaviour

Heavily filled materials may exhibit yield behaviour, which implies that the material requires a stress greater than a limiting lower value (the yield stress τ_y) to overcome entanglement and/or interaction of fillers or destruction of networks before any flow will occur. However, Barnes et al [4] suggested that yield is a consequence of instrument limitations. In reality, yield stress can be a convenient way of describing apparent material behaviour on timescales appropriate to industrial processes.

Methods reported for determining yield stress [77] include extrapolation of controlled strain test data to zero-shear rate, or by using controlled stress measurements to identify the maximum stress at which the non-flow condition is still satisfied. Extrapolation of controlled strain rate data appears problematical as data for material in a flowing state are extrapolated to predict the behaviour of a material in a static state. For materials that exhibit yield it is most likely that the structure will change on commencement of flow and thus the grounds for extrapolation are suspect. Furthermore, the process of extrapolation to a zero-shear rate itself is problematical.

Controlled stress measurements require that the instrument is able to control stress at sufficiently low levels and for the displacement/strain measurement to have high-resolution capability. It reality it is only possible to state that the material does not have a yield stress at a certain value. The absence of measurable flow in a controlled stress measurement may solely mean that the displacement/strain was too small to measure in the timescale of the measurement, rather than their being a true yield behaviour.

For observing yield stress behaviour Dealy [22] suggested presenting data as viscosity versus shear stress. As the limiting shear stress is approached from above, the viscosity will increase significantly indicating a yield-type behaviour. Utracki [78] reported on the use of oscillatory shear storage and loss moduli, *G'* and *G''* respectively, for determining yield behaviour which

is identified by a plateau in values when plotted as a function of angular frequency at decreasing angular frequency. Similarly, Tsao et al [25] reported that Si powder filled polyethylene exhibited a yield stress, stating that the slope of the log (complex viscosity) versus log (frequency) of the filled polyethylene curves was –1 at low frequency thereby indicating a yield stress in the system.

Dealy [22] observed yield behaviour for talc, titanium oxide, calcium carbonate and carbon black filled materials, and found that yield stress increased exponentially with volume fraction. Shenoy [1] commented that particle size affected the yield stress, being larger for smaller particle sizes than large particle sizes. Yield stress for extensional flow was approximately √3 of that in shear. Wang [38] reported yield stress behaviour for calcium carbonate filled polypropylene above a critical volume fraction of approximately 20%. However, the yield stress values obtained from different test methods using a rotational rheometer differed by up to a factor of x10. This difference was attributed to the different characteristic times of the various test methods as yield was due to the breakdown and recovery of networks [38]. Utracki [78] reported that the yield stress could be fitted by

$$\tau_y = K(\phi - \phi_o)^n \tag{7}$$

where K, n and ϕ_o are constants and $\phi_o \approx 0$.

6 Constitutive equations

6.1 Shear Viscosity

This section presents some of the models used to describe the rheological behaviour of filled materials. Modelling of the rheological behaviour of filled systems has been reviewed in depth by Shenoy [1], Macosko [19], Jinescu [79] and Han [80].

Einstein's equation for a dilute suspension of rigid spheres in which there is no interaction of particles is given by:

$$\frac{\eta}{\eta_0} = 1 + 2.5\phi \tag{8}$$

where

η = viscosity of suspension of filler particles
η_o = viscosity of Newtonian liquid
ϕ = volume fraction of filler particle

This expression does not predict an infinite value of viscosity at the limiting filler content corresponding to the maximum volume fraction and it is noted that the viscosity of the suspension remains Newtonian. Barnes et al [4] commented that for dilute suspensions covering volume fractions below 10% the viscosity does not increase by more than 40% thus generally supporting this equation. Higher terms in the volume fraction have been proposed to take into account additional model features, i.e.:

$$\frac{\eta}{\eta_0} = 1 + \alpha_1\phi + \alpha_2\phi^2 + ... \quad (9)$$

As an example of this form of model, Shenoy [1] refers to the expression due to Thomas [81] for concentrated suspensions of uniform solid spheres of $0.15 < \phi < 0.6$:

$$\frac{\eta}{\eta_0} = 1 + 2.5\phi + 10.05\phi^2 + 0.00273\exp(16.6\phi) \quad (10)$$

Alternative forms that attempt to predict the behaviour as the phase volume approaches the maximum value have been developed. For example, for concentrations up to ϕ_m the following form has been used Eilers [82]

$$\frac{\eta}{\eta_0} = 1 + \frac{1.25}{\left(1 - \phi/\phi_m\right)} \quad (11)$$

which predicts that as ϕ tends to ϕ_m then the relative viscosity tends to infinity. A similar form for concentrated suspensions of uniform solid spheres with ϕ tending to ϕ_m reported by Shenoy [1] is the equation due to Frankel and Acrivos [83]:

$$\frac{\eta}{\eta_0} = 1 + \frac{9\left(\phi/\phi_m\right)^{1/3}}{8\left(1 - \phi/\phi_m\right)^{1/3}} \quad (12)$$

Numerous equations of this type have been proposed by various workers of which only a limited set of examples is given to illustrate the types of model available. The reader is referred to Shenoy [1], for example, for further details. Such equations are based on assumptions of shape and size distribution. However, equations for rod or elliptical shaped particles and for spherical particles with size distributions in Newtonian fluids are less well established.

A particular problem in using such equations is that it is not always possible to determine the maximum volume fraction of a filler type. Values have been derived for simple cases, for example Table 1, but for the majority of real materials in which more complex geometries or a particle size distribution exist, the determination of the maximum volume fraction is not always possible. It can be difficult to characterise the filler, let alone predict the theoretical maximum volume fraction.

Table 1 Maximum volume fraction for various filler geometries and packing arrays [3,4]

Particles/packing array	Maximum volume fraction
Cubic lattice, spheres	0.524
Random close packing of sphere	0.637
Hexagonally packed sheets just touching	0.605

Body centred cubic packing of sphere	0.68
Rods (L/D=30) – random packing	0.173
Rods (L/D=16) – random packing	0.303
Rods (L/D=8) – random packing	0.476

It is noted that uniform alignment of high aspect ratio particles increases the theoretical packing density and flow may increase or decrease the alignment of the particles. Furthermore, the use of filler with a distribution of sizes has a lower viscosity than one with single size for the same volume fraction. This is predicted, for example, by the MPK equation as the maximum volume fraction is higher for a filler having a size distribution. Similarly, agglomerations will affect the maximum volume fraction.

The Marron – Pierce – Kitano (MPK) expression has been proposed for extending the predictive capability to greater than dilute concentrations in Newtonian systems [84]:

$$\frac{\eta}{\eta_0} = \left[1 - \frac{\phi}{\phi_m}\right]^{-2} \tag{13}$$

where

η = viscosity of suspension of filler particles
η_o = viscosity of Newtonian liquid
ϕ = volume fraction of filler particles
ϕ_m = maximum volume fraction (at which $\eta \to \infty$)

and where the viscosity ratio η/η_o is determined for a given shear stress. This expression is simple to implement as a value for the maximum volume fraction can be simply determined from experimental data rather than being derived from a knowledge of the filler quantity and geometry. Re-arranging the expression yields:

$$\sqrt{\frac{\eta_0}{\eta}} = 1 - \frac{\phi}{\phi_m} \tag{14}$$

A plot of $\sqrt{\frac{\eta_o}{\eta}}$ versus ϕ has a gradient equal to $-1/\phi_m$ thus permitting easy determination of the maximum volume fraction by extrapolation given a limited amount of data. This approach of determining the maximum volume fraction using the MPK expression has the advantage, in addition to it not being used to easily predict the maximum volume fraction, that it is likely to compensate for errors in the application of the expression for predicting the effect of filler on viscosity. It does require, however, a small subset of data on which to base predictions and thus might not be so suitable for initial materials design, but more so for materials development.

Using the MPK equation, for two systems of differing volume fractions ϕ_1 and ϕ_2 a shift in the curves can be carried out using the following relation

$$\frac{\eta_1}{\eta_2} = \left[\frac{\phi_m - \phi_1}{\phi_m - \phi_2}\right]^{-2} \tag{15}$$

and the maximum volume fraction is given by:

$$\phi_m = \left[\frac{\phi_2 \left(\frac{\eta_1}{\eta_2} \right)^{1/2} - \phi_1}{\left(\frac{\eta_1}{\eta_2} \right)^{1/2} - 1} \right] \tag{16}$$

This process results in a so-called master curve for viscosity, when plotted as a function of stress (see Section 6.4), thus permitting prediction of the behaviour of materials with different loadings.

Barnes [15] presented significant evidence that a wide range of systems and fillers can be analysed using this approach to successfully yield a master curve. However, for fibre filled material the fit was not so satisfactory. A simple modification to the MPK equation of the form given by equation A2.1 has been investigates (Appendix 2), and found to give a significantly improved fit to data.

Barnes et al [4] and Hackley et al [5] reported on a further modification to the MPK equation of the form:

$$\frac{\eta}{\eta_0} = \left[1 - \frac{\phi}{\phi_m} \right]^{-[\eta]\phi_m} \tag{17}$$

where [η] is the intrinsic viscosity[3] and the factor $[\eta]\phi_m$ has a value ranging from approximately 1.9 to 2.8.

For further expressions modelling the effect of fillers on the shear viscosity of fluids the reader is referred to Shenoy [1], Macosko [19] Jinescu [79] and Han [80]. The principle difficulty is in knowing which model to select for a given material system, given that it is likely that all models fit certain materials and ranges of volume fraction reasonably well, given the complexity that is industrial filled materials.

6.2 Extensional flow

Modelling of extensional flows of filled materials has received considerably less attention than shearing flows. Shenoy [1] commented that, in comparison with shear flow characterisation, there is a dearth of work on the effect of filler parameters on extensional flow behaviour. This may well be due the fact that polymers predominantly used in extensional flow processes, e.g. film blowing, tend to be unfilled. A high level of filler will tend to result in a low strain failure of the material in extension [85]. A significant exception to this is in the flow of materials in converging sections, for example in the extrusion die head where the flow channel upstream of the die profile reduces in cross-sectional area.

[3] Intrinsic viscosity – the value of the reduced viscosity in the limit as the concentration approaches zero, the reduced viscosity being given by the difference between the suspension and solvent viscosities divided by the solvent viscosity.

Batchelor [34] and Goddard [35] clearly demonstrated in their modelling that the effect on extensional flow properties of high aspect ratio fillers in Newtonian and non-Newtonian fluids can be very significant. Batchelor [34] developed a theory to predict the effect of the addition of slender particles (rods) to a Newtonian fluid on its extensional flow behaviour. The model considers the contribution made by the fibres in perturbing the flow field – the fluid at a fibre wall having the same velocity along the whole length of the fibre. Goddard [35] subsequently developed a theory along similar lines but one that is applicable to non-Newtonian fluids. Both theories apply to concentrated suspensions of particles where the particles are aligned in the direction of extension. The theory developed by Goddard [35] predicts substantial differences in the extension flow behaviour of fibre-filled Newtonian and non-Newtonian fluids. For the non-Newtonian fluid model, shear thinning occurs in the region of high shear adjacent to the fibres resulting in a decrease in the additional tensile stress contribution due to the presence of the fibres compared with the Newtonian case. This modelling clearly suggests that the extensional flow properties will be strongly influenced by the orientation of particles. Experimental data produced by Mewis et al [86] on fibre filled Newtonian fluids were in agreement with the predictions of Batchelor [34].

6.3 Yield flow

As discussed in Section 5.6 the validity of yield stress is questioned. However, on a practical scale there is potential benefit in modelling yield behaviour, although for polymer processing the application of yield behaviour is probably limited given the nature of processing and timescales involved. Nevertheless, models that are used to fit apparent yield behaviour are presented below. For further details the reader is referred, for example, to Shenoy [1], Collyer [13] and Ferraris [20].

6.3.1 Bingham

$$\sigma = \sigma_y + \eta\dot{\gamma} \tag{18}$$

$$\dot{\gamma} = 0 \quad for \left| \sigma \right| < \left| \sigma_y \right|$$

where σ_y is the yield stress. This gives Newtonian behaviour above the yield stress.

6.3.2 Casson

$$\sigma^{1/2} = \sigma_y^{1/2} + C\dot{\gamma}^{1/2} \tag{19}$$

$$\dot{\gamma} = 0 \quad for \left| \sigma \right| < \left| \sigma_y \right|$$

where C is a constant. Dealy [22] commented that the Casson model gives a better fit to data than the Bingham model.

6.3.3 Herschel-Bulkley model

$$\sigma = \sigma_y + K\ \dot{\gamma}^n \tag{20}$$

$$\dot{\gamma} = 0 \quad for \left| \sigma \right| < \left| \sigma_y \right|$$

This model is the power-law viscosity model with a yield behaviour added and as such is not suitable for modelling material that exhibit a Newtonian plateau at low shear rates. Tang et al [87] demonstrated the estimation of the parameters of a Herschel-Bulkley fluid under wall slip conditions using a combination of capillary and squeeze flow viscometers. However, the squeeze flow data were analysed using finite element modelling, in an inverse problem approach, and the authors acknowledged that the uniqueness of the solution was a significant problem. Such an inverse analysis approach is a non-trivial exercise.

6.3.4 Modified Herschel-Bulkley model

The modified Herschel-Buckley model advances on the Herschel-Buckley equation in that it provides a power-law behaviour with yield but also a Newtonian plateau region η_N at low shear rates.

$$\eta = \frac{\sigma_y}{\dot{\gamma}} + \eta_N \left[1 - \left(\lambda\dot{\gamma} \right)^2 \right]^{(n-1)/2} \tag{21}$$

where

$$\dot{\gamma} = 0 \quad for \left| \sigma \right| < \left| \sigma_y \right|$$

6.3.5 Vom Berg /Ostwald-deWaele

Ferraris [20] presented the following expression by Vom Berg and Ostwald-deWaele [88, 89] used for describing the rheology of concrete:

$$\sigma = \sigma_y + B \sinh^{-1}(\dot{\gamma}/C) \tag{22}$$

where B and C are constants.

6.4 Unification of curves – Master curves

Czarneckie and White [27] reported that Vinogradov and Malkin [Z95] proposed presenting viscosity – shear rate data in the form

$$\eta(\dot{\gamma})/\eta_o \quad versus \quad \eta_o\dot{\gamma} \tag{23}$$

where η_o is the zero-shear viscosity and found reasonable superposition for glass fibre reinforced PS, cellulose and Kevlar reinforced PS , and silicone oil with glass fibres.

Lee et al [90] presented a unification of results for the shear viscosity of polyester sheet moulding compounds on the basis of the plotting:

$$\frac{\eta}{\eta_o} \quad versus \quad \frac{\dot{\gamma}\,\eta_o}{\sigma} \tag{24}$$

where η_o is the zero shear viscosity and σ is the shear stress.

Shenoy [1, 91] presented a unification of shear viscosity data for materials based on the use of the melt mass flow rate (MFR) value. He reported that by plotting:

$$log\ (shear\ viscosity \times MFR)\ \text{versus}\ log\ (shear\ rate / MFR) \tag{25}$$

a master curve is obtained for a given group of materials. Shenoy [1] also proposed a method that would take into account the measurement of melt flow rate (MFR) and shear viscosity data at different temperatures, but it requires knowledge of the glass transition temperature of the polymer. MFR values can be determined by measurement or by analysis of shear stress-shear rate data. The latter approach may be problematic as for low MFR materials data may not be available at sufficiently low shear stress values and extrapolation, which can be problematic, may be necessary to determine MFR values (an MFR of 10 g/cm^3 corresponds to an apparent shear rate of 2.3 s^{-1}). Shenoy [91] commented that a discrepancy at low rates between filled and unfilled materials in the master curve is due to the yield stress characteristic of the filled materials. At higher stresses the curves for the filled and unfilled materials tended to coalesce. The success of this approach is limited by the similarity of the materials being gathered in the master curve. It appears that the more similar the materials the better quality the master curve will result. Shenoy [91] added that the technique provides "order of magnitude information on viscosity, adequate for most exercises in process design, optimization and trouble shooting".

Individual master curves presented [1] for filled and unfilled LDPE, PP, PS, Nylons, PET, PC, PEI and PEEK showed the extent to which a master curve fitted all the data, that fit being good for PP, nylons, PC, PEI and PET and noticeably poorer for PS.

In oscillatory rheometry use in made of the empirical Cox-Merz relation to correlate dynamic viscosity η^* with steady shear flow viscosity η [92] thus:

$$\eta(\dot{\gamma}) = \left|\eta^*(\omega)\right| \qquad where\ \ \dot{\gamma}\ (s^{-1}) = \omega\ (rad.s^{-1}) \tag{26}$$

where $\dot{\gamma}$ is the shear rate and ω the angular frequency. The Cox-Merz [92] has been found to work well for unfilled materials but not for filled materials. [1, 38, 93]. Shenoy [1], reporting on Doraiswamy et al [94], commented that, instead of plotting the dynamic viscosity as a function of angular frequency, if it is plotted as a function of the product of angular frequency and maximum amplitude of oscillation then good agreement with steady shear viscosity plotted as a function of shear rate is obtained. Wang et al [38] commented that this modified Cox-Merx relationship was only valid for high loadings of filler, estimated by this author to be 20% or higher, and not at low shear rates (< 0.01 s^{-1}).

Shenoy (95) also presented further unification of rheological data for asphalt materials where the following are plotted

$$\frac{|G^*|}{Load}\ \ vs\ \ \frac{Frequency}{MVR} \tag{27}$$

where *Load* is the load used in the melt flow rate test and *MVR* is the melt-volume flow rate determined from the test.

On the issue of presentation of results, Barnes [15] pointed out that when plotting data for different filler loadings as a plot of log (shear viscosity) versus log (shear rate) the effect of different loading is typically to shift the curves in both the viscosity and rate directions. However, when plotting the data as log (shear viscosity) versus log (shear stress) the effect of different filler loadings is predominantly to shift the curves in the viscosity direction only, thus making visualisation of filler effects more obvious.

7 Summary

This report presents a review of measurement methods for the rheological, or flow, properties of filled materials focusing on polymeric materials and in particular on the measurement of slip flow that occurs in filled materials, predominantly through the development of a lubricating layer adjacent to the wall of the flow channel. It also describes models used for predicting the effect of filler on the viscosity of materials and presents the basis for unification of flow curves. The modelling and unification of flow curves can be used to facilitate the prediction and measurement of the rheological behaviour of materials.

8 Acknowledgement

The work reported in this paper was carried out as part of a programme of underpinning research supported by the Department of Trade and Industry on measurements related to the processability of materials.

9 References

1. A.V. Shenoy, Rheology of filled polymer systems, Kluwer Academic Publishers, 1999.
2. BS 5168: 1975 Glossary of Rheological Terms
3. Hadley, D.W. and Weber, J.D., Rheol. Acta, **14** (1975) pp.1098-1109.
4. Barnes H.A., Hutton, J.F. and Walters, K., Rheology Series, Vol. 3: An Introduction to Rheology, Elsevier, 1989.
5. Hackley, V.A. and Ferraris, C.F., Guide to Rheological Nomenclature: Measurements in Ceramic Particulate Systems, NIST Special Publication 946.
6. M. Rides and C.R.G. Allen, Extensional flow properties of polymer melts using converging flow methods, Measurement Good Practice Guide No.16, National Physical Laboratory.
7. Murty K.N. and Modlen, G.F., Polym. Eng. Sci., **17** No.12 (1977) pp.848-853.
8. Maschmeyer, R.O. and Hill, C.T., Trans. Soc. Rheol., **21:2** (1977) pp.183-194.
9. Coates, P.D., Kelly, A.L., Rose, R.M. and Woodhead, M., In-procxess shear flow measurements in extrusion and injection moulding, In-Process Measurement Series IMP1University of Bradford, ISBN 1 85143 171 3.
10. Macosko, C.W., Rheology – Principles, Measurements and Applications, VCH Publishers, 1994.
11. Silva-Nieto, R.J., Fisher, B.C. and Birley, A.W., Polym. Eng. Sci., **21** no. 8 (1981) pp. 499- 506.
12. Attanasio A., Bernini, U., Galloppo, P. and Segre, G., Trans. Soc. Rheol., **16:1** (1972) pp.147-154.
13. Collyer A.A. and Clegg, D.W., Rheological Measurement, Chapman & Hall, 1998.
14. Lauger, J., Muller, M. and Tyrach J., Applied Rheology, July/August 1999, pp.145-147.
15. Barnes H.A., A review of the rheology of filled viscoelastic systems, Rheology Reviews 2003, pp.1-36, Edited DM Binding & K Walters, The British Society of Rheology ISBN 0-9538904-8-1.
16. Rides, M Aspects of the rheology of unsaturated polyester dough moulding compounds, Ph.D. 1993, Brunel University.
17. Cross, M.M. and Kaye, A., Polym. Eng. Sci., **26**, No 2 (Jan 1986) pp.121- 126.
18. Cross, M.M. and Kaye, A., Polymer, **28** (1987) pp.435-440.
19. Macosko, C.W., Rheology – Principles, Measurements and Applications, VCH Publishers, 1994.
20. Ferraris, C.F., J. Res. Natl. Inst. Stand. Technol. 104, (1999) pp.461-478, Measurement of the Rheological Properties of High Performance Concrete: State of the Art Report, NIST, USA.
21. ISO 12058-1 Plastics -- Determination of viscosity using a falling-ball viscometer -- Part 1: Inclined-tube method.

22. Dealy J.M. and Wissbrun K.F., Melt rheology and its role in plastics processing - Theory and Application. Chapman and Hall, 1995, p. 340-341.

23. Ausias, G., Jego, M., Sepehr, M., Carreau, P.J., Fraissard, B., and Moan, M., Rheological properties of short fibre filled polypropylene in small amplitude oscillatory shear and in creep flows, Proceedings XIIIth International Congress on Rheology, Cambridge, UK, 2000.

24. Potente, H., and Cunha, R.V., Studies on flow of polymer melts with magnetic fillers in a magnetic field, Proceedings of Polymer Processing Society Conference PPS-18, Portugal, 16-20 June 2002.

25. Tsao, I.L., Metzner, A.B., and Danforth, S.C., Rheological study of highly filled molten polymer systems for injection molded ceramic-ceramic composites, 2nd Technical conference of the American Soc. for Composites, Delaware, 23-25 Sept 1987, pp.316-325.

26. Wang, Y., and Yo, M-J., Polymer Composites, **21:1** Feb 2000, pp.1-12.

27. Czarnecki, L. and White, J, J. Applied Polym. Sci., **25** (1980) pp.1217-1244.

28. Wang, Y. and Yu, M-J., Transient measurements for the thixotropic behaviours of highly filled polypropylene, Proceedings XIIIth International Congress on Rheology, Cambridge, UK, 2000.

29. M. Rides and C.R.G. Allen, Extensional flow properties of polymer melts using converging flow methods, Measurement Good Practice Guide No.16, National Physical Laboratory.

30. Cogswell, F.N., Polym. Eng. Sci., **12** No.1 (1972) pp.64-73.

31. Binding, D.M., J. Non-Newtonian Fluid Mech., **27** (1988) pp.173-189.

32. Binding, D.M., J. Non-Newtonian Fluid Mech., **41** (1991) pp.27-42.

33. Gibson, A.G., Composites, **20** No.1 (1989) pp.57-64.

34. Batchelor, G.K, J. Fluid Mech., **46** Pt 4 (1971) pp.813-829.

35. Goddard, J.D., J. Non-Newtonian Fluid Mech., **1** (1976) pp.1-17.

36. White, J.L., Czarnecki, I and Tanaka, H., Rubber Chem. Tech., **53** (1980) pp.823-35.

37. Walberer, J.A., and McHugh, A.J., J. Rheol. **45(1)** (2001) pp.187-201.

38. Wang, Y. and Wang, J-J., Polym. Eng. Sci. **39:1**, Jan 1999, pp.190-198.

39. Gahleitner, M. Bernreitner, K., Knogler, B. and Neiβl, W., Macromol. Symp., **108** (1996) pp.127-136.

40. Tuinier R. and Taniguchi T, J. Phys. Condens. Matter, **17** (2005).

41. M. Modigell, M. Hufschmidt, J. Koke, C. Heine, S. Han, S. Stapf, and J. Petera, Investigation of wall slippage in suspensions by NMR imaging, Proceedings XIIIth International Congress on Rheology, Cambridge, UK, 2000.

42. Yilmazer, U. and Kalyon, D.M., Slip effects in viscometric flows of highly filled suspensions, ANTEC 1989, pp.1682-1686.

43. Kalyon, D.M., J. Materials Proc. & Manufacturing Sci., **2** (1993) pp159-187.

44. Cohen, Y and Metzner, A.B., Rheol. Acta, **25** (1986) pp.28-35.

45. Thierty Aubry, Louis Blonce and Michel Moan, Apparent slip in the rheometry of an associative polymer solution, Proceedings XIIIth International Congress on Rheology, Cambridge, UK, 2000.

46. Chen, Y, Kalyon, D.M. and Bayramli, E., ANTEC, 1992, pp.1747- 1751.

47. Piau, J-M., Kissi, N. and Mezghani, A., J. Non-Newt. Fluid Mech., **59** (1995) pp.11-30.

48. Mooney, M., J. Rheology, April 1931, pp.210-222.

49. Yoshimura, A.S. and Prud'homme, R.K., SPE Reservoir Engng., May 1988 pp.735–742.

50. Arturo F. Mendez-Sanchez, Ma. Del Rosario Lopez-Gonzalez, Jose Perez-Gonzalez, and Lourdes de Vargas, Flow instabilities and the presence of positive and negative slip in micellar systems, Proceedings XIIIth International Congress on Rheology, Cambridge, UK, 2000.

51. Jean L. Leblanc and Thoranit Navarat, Assessing the wall slip rate of complex polymer systems with the Mooney method, Proceedings XIIIth International Congress on Rheology, Cambridge, UK, 2000.

52. B. Hagström, Measurement of Wall Slip for a PVC Compound and its Application in CFD Simulations of a Melt Distributor in a Pipe Die. [239] Proceedings of Polymer Processing Society Conference PPS-18, Portugal, 16-20 June 2002.

53. Fleming D., Progress in Rubber and plastics Technology, **15** No.4, 1999, pp.215-233.

54. Geiger, K., Kautsch Gummi Kunstoffe, **43** (1989) pp.273-283.

55. Weigreffe, S., Kautsch Gummi Kunstoffe, **44** (1991) pp.216-221.

56. Mourniac, P.H., Agassant, J.F. and Vergnes B., Rheol. Acta, **31** (1992) pp.565-574.

57. Hatzikiriakos, S.G., Polym. Eng. Sci., **34** (1994) 19.

58. Lau H.C. and Scowalter, W.R, J. Rheol., **30** (1986) 193.

59. Hill, D.A, Hasegawa, T. and Denn, M.M., J. Rheol., **34** (1990) p891

60. Kalyon D.M., Gokturk, H. and Boz, I., An adjustable gap in-line rheometer, Highly Filled Materials Institute, Hoboken, NJ 07030.

61. Henson, D.J. and Makay, M.E., J Rheol., **39** (1995) p359.

62. Sanghyun Park, Seunghee Ryu and Chongyoup Kim, Apparent wall-slip in concentrated suspension of non-colloidal particles in polymer solutions, Proceedings XIIIth International Congress on Rheology, Cambridge, UK, 2000.

63. Y.L. Yeow, H.L. Lee, A.R. Melvani and G.C. Mifsud, Obtaining the Shear Stress-Shear Rate and Wall Shear Stress-Slip Velocity Relationships of Polymer Melts from Capillary Viscometry Data. [020] Proceedings of Polymer Processing Society Conference PPS-18, Portugal, 16-20 June 2002.

64. Yilmazer U and Kalyon, DM, J. Rheol. **33**(8) (1989) pp.1197-1212.

65. Jiang, T.Q., Young, A.C., and Metzner, A.B., Rheol. Acta, **25** (1986) pp.397-404.

66. B. Haworth, S.W. Khan and M. Guinebaud, Wall Slip and Injection Moulding of Particle-Filled Thermoplastics: Effects of Filler Coatings and Particle Dispersion.

[134] Proceedings of Polymer Processing Society Conference PPS-18, Portugal, 16-20 June 2002.

67. S. Ahn, and J.L. White, Influence of Low Molecular Weight Additives on the Die Extrusion of Thermoplastic Melts. [015]. Proceedings of Polymer Processing Society Conference PPS-18, Portugal, 16-20 June 2002.
68. Knappe, W. and Krumbock, E., Rheol. Acta, 25 (1986) pp.296-307.
69. A note on slippage during rheological measurements on concentrated dispersions, Malvern Instruments Application Note MAK507-01.
70. I Szarvasy, and J.F.T. Pittman, Pressure Drop and Die Surface Changes in uPVC Extrusion [305]. Proceedings of Polymer Processing Society Conference PPS-18, Portugal, 16-20 June 2002.
71. J. Graczyk, H. Buggisch, Capillary rheometry study of paste wall slip, Proceedings XIIIth International Congress on Rheology, Cambridge, UK, 2000.
72. Gleissle W and Windhab, E., Experiments in Fluids, **3** (1985) pp.177-180.
73. ISO 11443 Plastics – Determination of fluidity of plastics using capillary and slit-die rheometers.
74. Brydson, J.A., Flow Properties of Polymer Melts. George Godwin Ltd, London, Second Edition 1981.
75. Atwood, B.T. and Schowalter, W.R., Rheol. Acta, **28** (1989) pp.134-146.
76. Piau, J-M., Kissi, N. and Mezghani, A., J. Non-Newt. Fluid Mech., **59** (1995) pp.11-30.
77. Alderman, N., Applied Rheology Newsletter, An update on yield stress, Dec 1991, Warren Spring Laboratory.
78. Utracki, L.A., Polym. Comp., **7** (1986) pp.274-282.
79. Jinsecu, V.V., International Chemical Engineering, 14:3 (1974) pp.374-420.
80. Han, C.D., Multiphase Flow in Polymer Processing, Academic Press, 1981.
81. Thomas, D.G., Colloid Sci., 20 (1965) pp267-277.
82. Eilers, H., Kolloid Zh., 97 (1941) p.313.
83. Frankel, N.A. and Acrivos, A., Chem. Eng. Sci., 22 (1967) pp847-853.
84. Kitano, T., Kataoka, T. and Shirota, T., Rheol. Acta, **20** (1981) pp.207-209.
85. White, J.L., and Tanaka, H., J. Applied Polym. Sci., **26** (1981) pp.579-589.
86. Mewis, J. and Metzner A.B., J Fluid Mech., **62** (1974) pp.593-600.
87. Tang H.S. and Kalyon, D.M., Rheol. Acta, **43** (2004) pp.80-88.
88. W. von Berg, Influence of specific surface and concentration of solids upon the flow behavior of cement pastes, Mag. Concrete. Res., **31** (1979) pp.211-216.
89. Tattersall, G. H., The workability of concrete, a viewpoint Publication, PCA 1976.
90. Lee, L.J., Marker, L.F. and Griffith, R.M., Polymer Composites, **2** No.4 (1981) pp.209-218.

91. Shenoy, A.V., Saini, D.R. and Nadkarni, V.M., Polymer Composites, **l4** No.1 **(**Jan 1983) pp.53-63.

92. Cox, W.P. and Merz E.H., J. Polym. Sci., **28** (1958) No 118 pp.619-622.

93. Kitano, T., Nishimura, T., Kataoka, T. and Sakai, T., Rheol. Acta, **19** (1980) pp.617-673.

94. Doraiswamy, D., Mujumadar, A.N., Tsao, I., Beris, A.N., Danforth S.C. and Metzner A.B., J Rheol., **35** (1991) pp.647-85.

95. Shenoy, A., ASCE J. Materials in Civil Engineering, **13** (2001) pp.260-273.

96. Rabinowitsch, B., Z. Physik Chem., **A145**, 1 (1929) pp.1-26.

97. Lupton, J.M. and Regester, J.W., Polym. Eng. Sci., **5** (1965) pp.235-245.

Appendices

Appendix 1: Theory for the determination of slip velocity by capillary rheometry following the Mooney approach

The analysis of capillary die extrusion rheometry experimental data is presented here for the determination of slip velocity, following the approach first proposed by Mooney [48]. The term "slip" has been used here to signify either a large velocity change near the wall that could be attributed to either a thin, high shearing layer with zero wall velocity, or to a non-zero wall velocity.

Slip flow can be modelled by the addition of a slip flow velocity to the shear flow velocity profile. This assumes that the slip layer can support a shear stress that is necessary for the shear flow to occur. To maintain continuity:

$$Q_T = Q_{shear} + Q_{slip} \tag{A1.1}$$

where the subscripts *T*, shear and slip represent the total flow rate and the shear and slip flow components of the total flow rate respectively. For flow in a capillary die of radius R the slip-flow flow rate Q_{slip} is given by:

$$Q_{slip} = u_s \, \pi R^2 \tag{A1.2}$$

where u_s is the slip velocity.

By definition, shear viscosity η is the ratio of shear stress σ to shear-rate $\dot{\gamma}$:

$$\eta = \frac{\sigma}{\dot{\gamma}} \tag{A1.3}$$

The shear viscosity power-law model can be written as:

$$\eta = K \, \dot{\gamma}^{n-1} \tag{A1.4}$$

where *K* and *n* are constants. For a power-law fluid the true wall shear-rate $\dot{\gamma}_w$ for flow in a cylindrical die (based on the true velocity profile of a power-law fluid rather than on that of a Newtonian fluid) is given, according to Brydson [74] (based on Rabinowitsch [96]) by:

$$\dot{\gamma}_w = \left[\frac{3n+1}{4n} \right] \frac{4Q}{\pi R^3} \tag{A1.5}$$

Using the above equations the following expression for the total flow rate in the presence of slip can be derived:

$$Q_T = \left[\frac{n\pi R^3}{3n+1}\right]\left[\frac{\sigma_w}{K}\right]^{1/n} + u_s \pi R^2 \qquad \text{(A1.6)}$$

This expression predicts that a plot of log Q_T versus log σ_w will not necessarily give a straight-line fit as would be the case for a power-law fluid with a slip velocity of zero. The dependence of the slip velocity u_s on wall shear stress will determine the shape of the plot.

$$\frac{4Q_T}{\pi R^3} = \left[\frac{4n}{3n+1}\right]\left[\frac{\sigma_w}{K}\right]^{1/n} + \frac{4u_s}{R} \qquad \text{(A1.7)}$$

If the wall shear stress is constant and assuming n does not vary, then:

$$\frac{4Q_T}{\pi R^3} = \text{constant} + \frac{4u_s}{R} \qquad \text{(A1.8)}$$

This expression predicts that, for a given wall shear stress, a plot of apparent wall shear-rate $4Q_T/\pi R^3$ versus $1/R$ will have a gradient of $4u_s$ thus enabling the slip velocity to be determined.

Appendix 2: Modified MPK equation

Fitting the MPK equation to shear viscosity data for a fibrous filler did not result in a good master flow-curve, Figure A2.1. In this figure the experimental data are presented as points and the reduced shear viscosity values calculated using the MPK equation are plotted as continuous lines. A good fit of the model would have resulted in the reduced shear viscosity data falling on a master curve that overlapped the shear viscosity data for the unfilled polymer. The poor reduction of experimental data to the unfilled material's values was considered to be due to the MPK equation not sufficiently taking into account the greater interaction between filler particles for fibre filled materials, compared with non-fibrous fillers. To address this, the sensitivity of the equation to increasing filler content was changed by adding an exponent term p to the 'volume fraction to maximum volume fraction' term of the MPK equation and also a rate dependence term n was added, Equation A2.1.

Assuming the form for the modified MPK equation:

$$\frac{\eta}{\eta_0} = \left[1 - \left(\frac{\phi}{\phi_m}\right)^p\right]^{-2n} \quad for\ \eta\ (\sigma_1), \eta_o(\sigma_1) \qquad \text{A2.1}$$

where n is the slope of the log (shear stress) versus log (shear rate plot) and p is a constant, re-arranging gives:

$$1 - \left(\frac{\eta}{\eta_0}\right)^{\frac{1}{-2n}} = \left(\frac{\phi}{\phi_m}\right)^p \qquad \text{A2.2}$$

Thus, taking logarithms yields:

$$\log\left[1 - \left(\frac{\eta}{\eta_0}\right)^{\frac{1}{-2n}}\right] = p \log\left(\frac{\phi}{\phi_m}\right) \qquad \text{A2.3}$$

or

$$log\left[1-\left(\frac{\eta}{\eta_0}\right)^{\frac{1}{-2n}}\right] = p\,log\,\phi - p\,log\,\phi_m \qquad \text{A2.4}$$

Thus a plot of

$$\log\left[1-\left(\frac{\eta}{\eta_0}\right)^{\frac{1}{-2n}}\right] \; versus \;\; \log\phi \qquad \text{A2.5}$$

has a gradient of p and an intercept value I_{nt} where:

$$I_{nt} = -\,p\;log\;\phi_m \qquad \text{A2.6}$$

The values for n and ϕ_m can be determined locally thus allowing variation in their values with shear rate or stress. This is particularly relevant to n, but for ϕ_m is more debatable. The effect of the additional terms is demonstrated in Figures A2.2 to A2.4 using data for PS/Kevlar at 180 °C from figure 13 of Czarnecki et al [27]. The following empirical equation was used to fit the shear viscosity data:

$$\eta_1 = \frac{A}{1+(B\sigma)^c} \qquad \text{A2.7}$$

The use of the normal MPK equation did not result in a sufficiently large scaling effect to reduce the data to a master curve. The use of the exponents p and n in the modified MPK equation resulted in a significantly improved master curve. However, by allowing the term ϕ_{max} to vary and be determined for a given shear stress, the fit to a master curve is improved further for volume fractions up to and including 10%. In both these latter cases the fit for the 20% volume fraction was relatively poor. This may be due to the greater interaction occurring at such high loads.

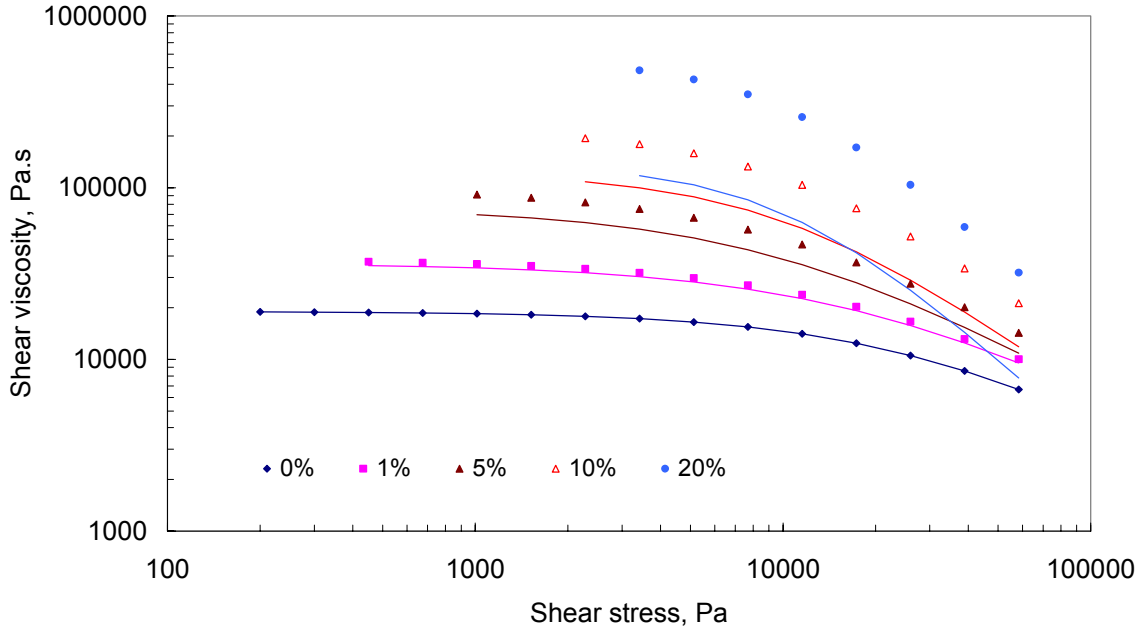

Figure A2.1. Reduction of shear viscosity for filled materials using equation A2.1, assuming n =1, p = 1 and ϕ_m = 0.307 (average value) - i.e. unmodified MPK expression.

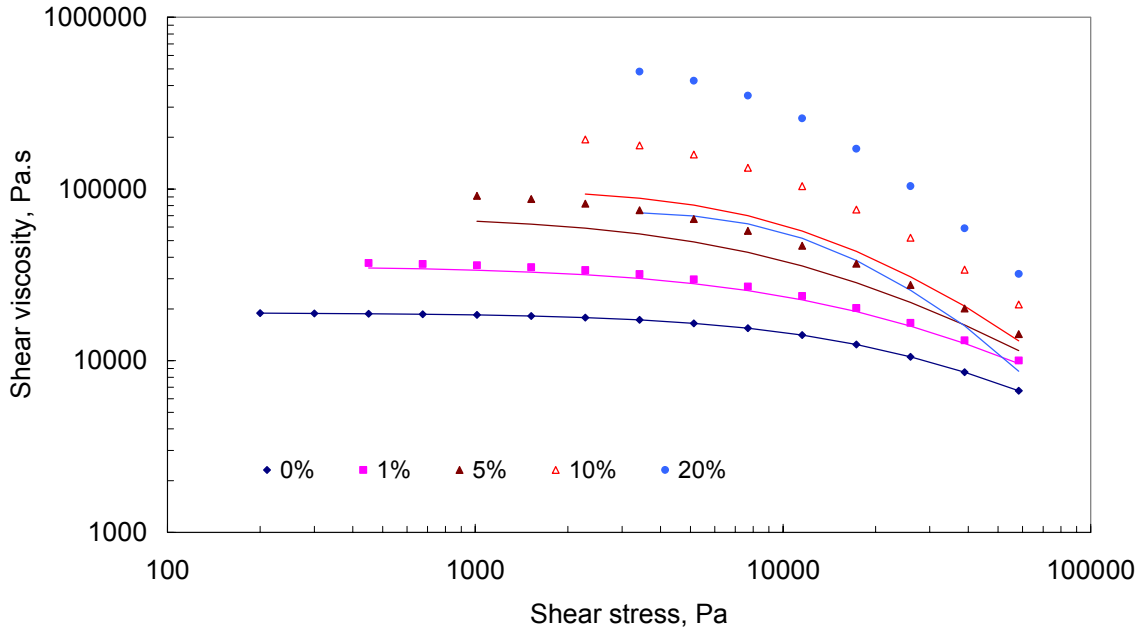

Figure A2.2. Reduction of shear viscosity for filled materials using equation A2.1, assuming n value calculated locally as a function of shear rate for the unfilled material, p = 1 and ϕ_m = 0.307 (average value)

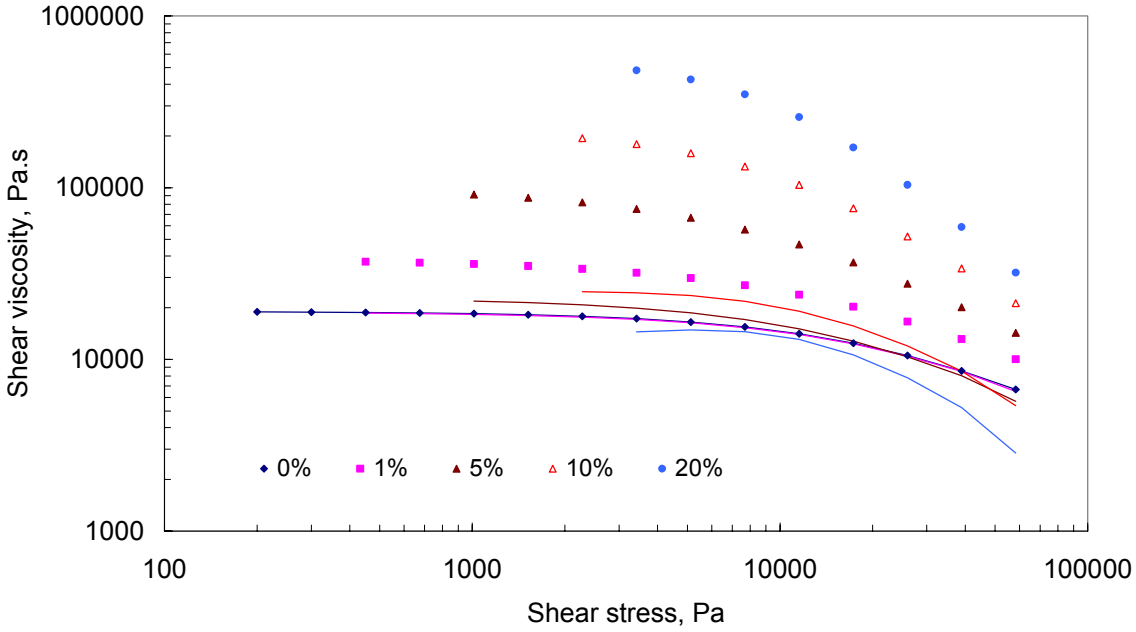

Figure A2.3. Reduction of shear viscosity for filled materials using equation A2.1, assuming p = 0.357, n calculated locally as a function of shear rate for the unfilled material and ϕ_m = 0.307 (average value with stress)

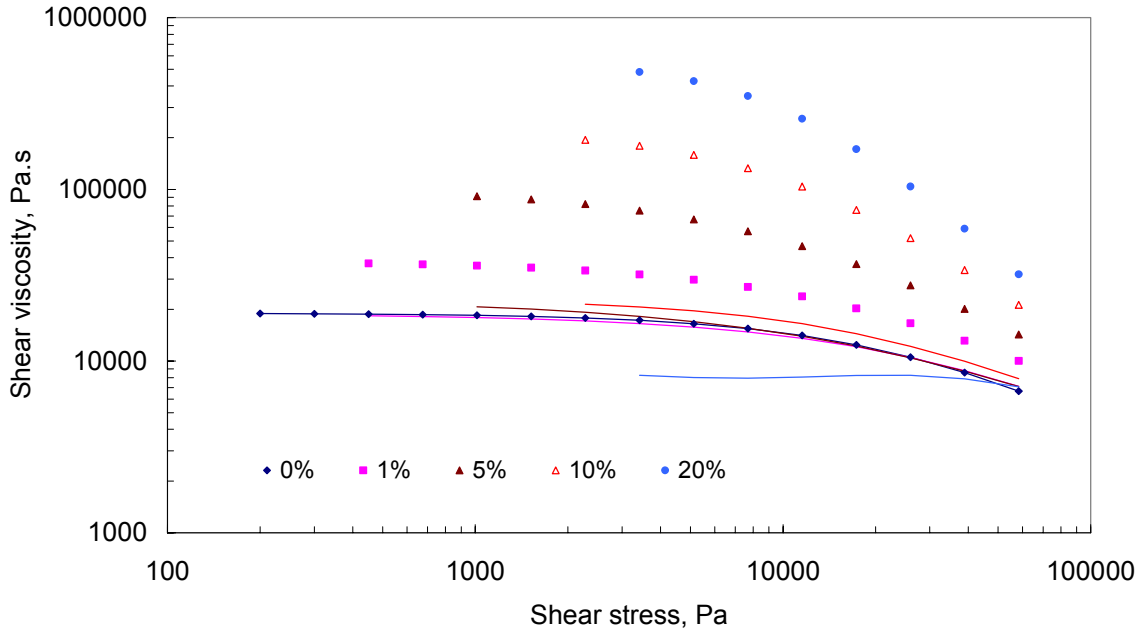

Figure A2.4. Reduction of shear viscosity for filled materials using equation A2.1, assuming n value calculated locally as a function of shear rate for the unfilled material, p = 0.357 and variable ϕ_m (decreasing from 0.3 to 0.2 with increasing stress).